Analytical approach for investigation of Hollow Cathode Orifice

Fabio Coccaro [(1)], Alessio Di Iorio[(1)], Franco Bosi[(2)], Alexander Daykin-Iliopoulos [(2)(3)], Igor O. Golosnoy[(3)], Steve B. Gabriel[(3)]

[(1)] Alma sistemi srl, Via Tenuta del Cavaliere 1- B, Guidonia (Rm) Italia, Email: fco@alma-sistemi.com
[(2)] Mars Space ltd, Unit 61/63 Basepoint Business Centre, Anderson Road, Southampton, SO14 5FF, United Kingdom, Email: franco.bosi@mars-space.co.uk
[(3)] University of Southampton, B20 TDHVL, University Road, Southampton, SO171BJ, United Kingdom, Email: I.Golosnoy@soton.ac.uk; sbg2@soton.ac.uk

Nomenclature

$A(z)$	Orifice cross section	$[m^2]$
B, c_1, c_2, c_3, C	Constants defined for general solutions	[-]
D_a	Ambipolar diffusion rate	$[m^2 s^{-1}]$
E_i	Xenon first ionization energy, 12.1	$[V]$
E_z	Axial electric field strength	$[V m^{-1}]$
e	Electron charge, 1.6×10^{-19}	$[C]$
$f_1(z), f_2(z)$	Auxiliary functions	[-]
I_e	Electron current	$[A]$
J_0, J_1	Zero-order and first order Bessel function	[-]
j_e	Electron current density	$[A m^{-2}]$
k	Boltzmann constant,1.38×10^{-23}	$[J K^{-1}]$
L	Orifice length, 7.5×10^{-4}	$[m]$
m_e	Electron mass, 9.11×10^{-31}	$[kg]$
m_i	Xenon mass, 2.20×10^{-25}	$[kg]$
$\dot{m}$	Mass flow	$[kg s^{-1}]$
n	Plasma number density	$[m^{-3}]$
n_e, n_i, n_n	Electron, ion, neutral number densities	$[m^{-3}]$
$n_\perp(0)$	Number density at centerline	$[m^{-3}]$
$n(0), n_n(0)$	Plasma and neutral number density at the orifice entrance	$[m^{-3}]$
$\bar{n}$	radially averaged ion number density	$[m^{-3}]$
$\dot{n}$	Ion generation rate	$[m^{-3} s^{-1}]$
P_j	j-species pressure	$[Pa]$
R	Original orifice radius 1.4×10^{-4}	$[m]$
r	Radial coordinate	$[m]$
T	Gas temperature in K	$[K]$
T_j	j-species temperature in eV	$[eV]$
u_j	j-species velocity	$[m s^{-1}]$
$u_{j,z}$	Axial component	$[m s^{-1}]$
$u_{j,\perp}$	Radial component	$[m s^{-1}]$
$u_{n,0}, u_{n,end}$	Neutral velocity at channel extremes	$[m s^{-1}]$
z	Axial coordinates	$[m]$
α	Degree of ionization	$[-]$
ζ	Viscosity	$[Pa \cdot s]$
η	Plasma resistivity	$[V m A^{-1}]$
λ_{01}	First zero of zero order Bessel function,2.4048	$[-]$
π	3.14159265358979323846…	$[-]$
$\sigma_{en}(T_e)$	Maxwellian averaged electron–neutral collision cross section	$[m^2]$
σ_{CEX}	charge exchange cross section, 1.4×10^{-18}	$[m^2]$
$\sigma(T_e)$	Maxwellian averaged ionization cross section	$[m^2]$
ν_{in}	Ions-neutral collision frequency	$[s^{-1}]$
ν_{en}	Electrons-neutral collision frequency	$[s^{-1}]$

KEYWORDS: hollow cathode, orifice, Electric propulsion life modelling.

ABSTRACT:

Prediction of hollow cathode orifice is one of the most important goals of a well performed design; engineers need simple design tools for a quantitative prediction of the orifice erosion. A recent work [1] suggests the use of an analytical solution in contrast to two-dimensional numerical models, generally very hard to develop. In this work, a global model is coupled with an analytical orifice model. The orifice model solves a simplified quasi-one dimensional flow with the use of mass balance for each species, diffusion drift equation in the radial direction and convection drift equation for ions in axial direction. The use of Dirichlet boundary conditions for plasma and neutral densities, extracted current and plasma potential allows for a full characterization of quantities involved in the erosion sputtering of the orifice wall.

Comparison are given with experimental data and existing literature for neutralizer NSTAR [2] at full power with extracted $3.26A$ and mass flow of $3.7 \times 10^{-7} kg/s$.

1. Introduction

The hollow cathode (HC) is a special type of cathode widely used in electric propulsion systems. For example, two HCs are used in direct current (DC) discharge ion thrusters, while HC neutralizers are used for any thruster that produces an ion beam[3]. In addition to the importance of HCs in terms of convention electric propulsion (EP) [4], there is also much interest in the use of HCs as plasma sources for a wide range of applications; from laser applications [5] to surface modification [6]. In the H2020 PATH project [7], HCs are being investigated as plasma sources for plasma antennas. Plasma antennas do apply plasma discharges either as an EM reflector or as radiating elements and introduce reconfigurable capabilities that are not achievable by conventional antennas. In order to operate properly, it is required a plasma density in the order of $\sim 10^{20} m^{-3}$. Preliminary tests (not yet published) show good results in achieving high-density

discharges with the use of HCs. Even though plasma antennas HCs and EP HCs work in different

A hollow cathode is essentially an open ended cylinder with a constricted end: the orifice. Neutral gas is injected in the tube. During the operation, a plasma is present in the enclosed region, usually referred to as insert region. Plasma is then extracted by the use of an external anode; an extra electrode – referred to as keeper – is added in the system for starting up procedures and overall protection of the system from the high-energy ion bombardment.

A critical component of the HC design is the orifice geometry; it dictates the insert pressure, and consequently plasma density and temperature. The erosion seems to be more predominant in small-size orifices, mainly due to high dense plasma and high sheath-potential that accelerate a high energy ion flux on the wall causing thermal-stimulated erosion and material sputtering [8].

And while there are many models for HC operational work, few of them try to account for the erosion of the orifice channel. It is not completely understood how the changing shape of the orifice influences the overall HC life-time, operational parameters and plasma properties. The erosion prediction is very complex, mainly due to high expenses of long-time running experiments required for visible erosion to happen, and due to the high computational expenses to account for all the physical phenomena happening in the orifice channel.

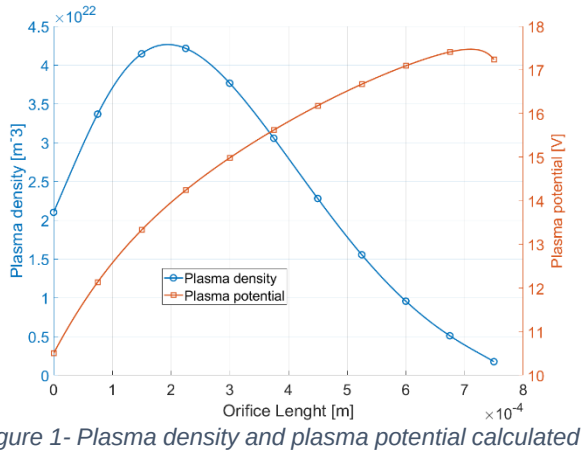

Figure 1- Plasma density and plasma potential calculated for NHC [9]*; the combination of the two is believed to be the main contributor to the erosion of the orifice channel*

Several authors gave important contributions in order to explain -qualitatively and quantitatively- what are the causes and how to predict the erosion. The research of Katz et al. [10] has been concerned with the development of a quasi-1D model of the HC suggesting that the erosion is mainly due to the peak in plasma density and the increasing sheath potential. Moreover, the importance of charge-exchange (CEX) collisions is recognized as essential to understand the behaviour of HC. In contrast to the simplified one-dimensional model, Mikellides et al. [9] and Sari et al. [11] developed a fully two-dimensional numerical model able to describe the whole HC system. The results of these groups correlate well with experimental measurements [12][13]; however such models are complex to develop and resource consuming.

The objective of this paper is to study the one-dimensional steady-state model of plasma flow process in the orifice of HCs following Katz et al. [10] approach, but revised with few further simplifications to allow for a more direct solution and to take account for the erosion that takes place over time. The use of none of the numerical techniques common in computational fluid dynamics (i.e. Finite volume element, finite differences) makes this model an alternative choice for cathode design. This simplified model could be helpful for a preliminary design of HC; due to its nature, it is trivial to reproduce, it is coupled with a global model and requires little computational resources.

To proceed we first formulate basic equations of mass balance plasma. Following the assumption of mixture of three species: neutrals, electrons and single charged ions, there are three such equations.

$$\iint_{\partial\Omega} n_j \boldsymbol{u_j} \cdot \boldsymbol{dA} = \iiint_{\Omega} \dot{n} dV \qquad (1)$$

Using the divergence theorem, (1) can be written in differential form:

$$\nabla(A u_n n_n) = -A\dot{n} \qquad (2)$$

$$\nabla(A u_i n) = A\dot{n} \qquad (3)$$

$$\nabla(A j_e) = Ae\dot{n} \qquad (4)$$

Finally, using radial diffusion to estimate fluxes on wall, the system (2-3-4) can be casted as quasi-one dimensional problem in $n(z), u_i(z), n(z), u_n(z), j_e(z)$ (plasma density, ions velocity, neutrals density, neutrals velocity, current density).

To have easier notation, from now on $\frac{d}{dz} = [-]'$.

$$[A u_n n_n]' = -A\dot{n} + \omega_{wall} n \qquad (5)$$

$$[A u_i n_i]' = +A\dot{n} - \omega_{wall} n \qquad (6)$$

$$[I_e]' = eA\dot{n} \qquad (7)$$

Where the wall losses coefficient ω_{wall} is derived in next sections. The electric current, ignoring ion transport, is defined as:

$$j_e \coloneqq e u_e n_e \quad I_e \coloneqq A j_e$$

As results of high plasma potential values near the wall, the losses due to electron flow to the wall is negligible when compared to the axial flow [9].

The ion-generation rate is

$$\dot{n} \coloneqq 4\sigma(T_e)n_n n\sqrt{\frac{eT_e}{2\pi m_e}} = K_{iz}(T_e)nn_n \qquad (8)$$

The impact ionization cross section for xenon averaged over a Maxwellian distribution of electrons at temperature T_e (expressed in *eV*) is [10]

$$\sigma(T_e) \approx 10^{-20}\left[3.97 + (0.643T_e) - (0.0368{T_e}^2)\right]\exp(-E_i/T_e) \qquad (9)$$

2. Orifice Model

Every mathematical model reproduces to a certain degree the relationships among the involved variables during the real phenomena. Arguably, numerical methods are more generally applicable than analytical or approximated methods. However, analytical solutions, when available, have the advantage to provide greater insight on the involved phenomena. It allows verifying the behaviour, shapes, and limits provided by the quantities involved. Moreover, simple solutions are needed to certification of convergence robustness and precision of numerical tools.

2.1. Assumptions

The possibility of an analytical solution is, in general, not guaranteed; the orifice problem allows for one, provided the following assumptions are made.

Plasma quasi neutrality and single charged ions are assumed; ions and neutrals are in thermal equilibrium.

The role of large CEX free-mean path is recognized as that of a primary contributor to plasma profile and loss rates [3]. Due to the CEX collisions it's believed that the heavy particles are able to reach thermal equilibria, while the electrons have a much larger temperature.

Steady-state and negligible Ions and electros inertia

Steady-state is assumed, and the erosion is calculated with a chosen time-step. The un-steady flow that appears due to the sudden change of geometry caused by the erosion is ignored as it is believed that the flow reaches steady-state fast. The erosion is considered to be a slow process that does not affect the plasma-fluid behaviour in the short time scale. Figure 2 shows the flow chart of how model works. Moreover, the inertia is assumed negligible in order to further simplify momentum equations for charged species.

All species' temperatures are considered constant along the orifice channel.

Previous numerical simulations [9][11][14] have shown that temperature gradients are considerably lower when compared to density variations. In order to simplify our model, we assume the electrons and gas temperatures constant along the orifice channel.

All quantities are considered constant in the radial direction.

This approach is usually known as quasi 1D or plug reactor. It is a sever assumption and it ignores the effect of radial gradients.

Ambipolar diffusion constant along the z-axis

This is very hard to achieve. As shown later the ambipolar diffusion will depend on $\sim 1/n_n$ and therefore increases as the density decreases. An average neutral density to estimate D_a is used in order to achieve a simpler solution.

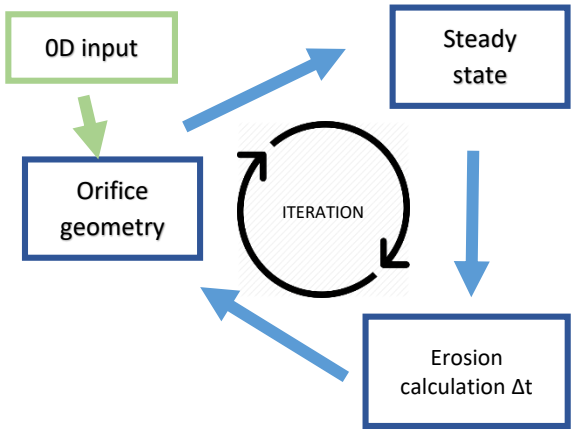

Figure 2 – orifice model flow chart. Input quantities are given from 0D-Global model. The model calculates the erosion rate for a given Δt; update the eroded radius and iterate assuming steady state flow.

Convective-controlled ion-flow in the axial direction.

As shown later, the ion flux will be mainly controlled by a diffusion term due to plasma density gradient, and a convective terms involving electron flux and neutral drag. The first being much smaller than the others [9] (and calculated to be few order of magnitude lower than convective terms) allows us to reduce the problem to a first order non-linear differential equation. The main consequence of this is that our solution will show sharper chances in quantities profiles. Nonetheless, it is a common assumption in all fluid problems with high velocity fluid flow.

Choked flow.

As the neutrals are affected by many different phenomena such as heating from the electrons, collisions, recombination, compressibility and friction with the wall, understanding the type of flow inside the orifice can be quite challenging. there is no easy way to obtain both an accurate neutral velocity profile and a simple solution for the orifice erosion. In this work, as done in all but full two-dimensional models, choked flow is assumed with sonic velocity at the exit of the orifice channel. This assumption is maintained also in the case of eroded channel. A simplifying Poiseuille's neutrals' velocity $u_n(z)$ is investigated in later section in order to show

the effect of neutrals' velocity profile on plasma quantities and erosion. Obviously, this is a severe assumption and more work is needed to relax it.

2.2. Boundary conditions and orifice input

The differential equations system (5-6-7) will require a number of boundary conditions and inputs to be solved.

As shown later, using the species momentum equation is possible to reduce the system to four unknowns: $n(z), n_n(z), j_e(z), u_n(z)$. Unfortunately, the system is underdetermined. For simplicity, we complete it assuming the neutrals' velocity to be known, letting us to obtain a general solution that depends only on the geometry and neutrals' velocity. Later, some a simple neutrals' velocity is proposed and discussed.

In order to run, the orifice model requires average electron temperature of the orifice region; plasma density, neutrals density and plasma potential at the entrance of the orifice channel. All of these, obtained with the use of a 0D model of the insert region, developed following the existent literature [3].

The mass flow entering the hollow cathode is used to estimate the velocity at the orifice entrance using:

$$u_{n,0} = \dot{m}/m_i A(0)(n_n(0) + n(0)) \tag{10}$$

And, finally, orifice geometry and extracted current.

2.3. Ion and electron momentum equation

Considering all the assumptions, the momentum equation for ions results as:

$$0 = -\nabla P_i - n m_i(\nu_{ie}(u_i - u_e) + \nu_{in}(u_i - u_n)) \tag{11}$$

For electrons:

$$0 = -\nabla P_e - n m_e(\nu_{ei}(u_e - u_i) + \nu_{en}(u_e - u_n)) \tag{12}$$

Where for electron-neutrals' collisions [15]

$$\nu_{en} \coloneqq \sigma_{en}(T_e) n_n \sqrt{eT_e/m_e} \tag{13}$$

$$\sigma_{en}(T_e) \approx 6.6 \times 10^{-19} \frac{T_e/4 - 0.1}{1 + (T_e/4)^{1.6}} \tag{14}$$

While the ions-neutrals collisions are controlled by Ions-neutrals charge-exchange collisions [16]

$$\nu_{in} \coloneqq n_n \sigma_{CEX} \sqrt{eT_i/m_i} \tag{15}$$

In the gas temperature range in study the cross section is considered $\sigma_{CEX} \approx 1.4 \times 10^{-18}$

Since $u_e \gg u_n$ and $m_i \nu_{ie} \approx m_e \nu_{ei}$, using the ideal gas law, the sum of the two momentum equations leads to:

$$u_i n = -D_a \nabla n - \frac{m_e \nu_{en}}{m_i \nu_{in}} \frac{j_e}{e} + n u_n \tag{16}$$

Where $D_a \coloneqq {k(T_i + T_e)}/{m_i \nu_{in}}$ is the ambipolar diffusion coefficient. By evaluating the terms with data from literature, it's found that the diffusion term is several order lower than the convective terms and therefore neglected in the axial direction, allowing us to simplify the model.

2.4. Radial flux

Following the very same approach of Katz et al. [10], the diffusion loss rate is set equal to the ion production rate, since electric current and neutrals flow are predominantly axial:

$$-\nabla[D_a \nabla n] = \dot{n} \tag{17}$$

Ignoring the radial neutrals density gradient and radial variation in temperature the radial plasma profile is obtained as zero-order Bessel function.

$$n(r) = n_\perp(0) J_0(Br) \tag{18}$$

$$B^2 = K_{iz} \bar{n}_n \tag{19}$$

Where an average neutrals density is used for both D_a and the ionization rate to further simplify the problem.

The radially averaged ion density is related to the ion density on the centerline by

$$\bar{n} = \frac{2\pi n(0)}{\pi R^2} \int_0^R J_0\left(\frac{\lambda_{01}}{R} r\right) r dr \tag{20}$$

And the ion flux at the wall is

$$\begin{aligned} -D_a \frac{\partial n}{\partial r} &= n(0) D_a J_1(\lambda_{01}) \lambda_{01}/R \\ &= \bar{n} D_a (\lambda_{01})^2/2R \\ &\equiv \bar{n} u_\perp \end{aligned} \tag{21}$$

Finally, the flux integrated over the wall is

$$\omega_{wall} n = 2\pi R u_\perp n = \pi D_a (\lambda_{01})^2 n \tag{22}$$

2.5. Governing equations

It is possible to solve (5-6-7) directly for densities, however switching to the ionization degree $\alpha(z) = n/(n + n_n)$ allows for a more elegant solution.

Using (16) in (6)

$$\begin{aligned} \left[A\left(-D_a \nabla n - \frac{m_e \nu_{en} j_e}{m_i \nu_{in} e} + n u_n\right)\right]' \\ = A\dot{n} - \omega_{wall} n \end{aligned} \tag{23}$$

Using the assumption of predominantly convection, the diffusion coefficient is neglected. With the use of (7)

$$[n u_n]' = A\left(1 + \frac{m_e \nu_{en}}{m_i \nu_{in}}\right)\dot{n} - \omega_{wall} n \tag{24}$$

And since $\frac{m_e \nu_{en}}{m_i \nu_{in}} \ll 1$, the system (5-6) becomes

$$[u_n n_n]' = -A K_{iz} n n_n + \omega_{wall} n \tag{25}$$

$$[u_n n]' = AK_{iz} n n_n - \omega_{wall} n \tag{26}$$

Whose sum leads to

$$[Au_n(n+n_n)]' = 0 \tag{27}$$

With

$$\begin{aligned} Au_n(n+n_n) &= A(0)u_n(0)[n(0)+n_n(0)] \\ &=: C \end{aligned} \tag{28}$$

Using the ionization degree and (28)

$$\begin{aligned} n_n &= \frac{1-\alpha}{\alpha} n \\ n &= \frac{C}{Au_n}\alpha \end{aligned} \tag{29}$$

Finally

$$\begin{aligned} [\alpha]' &= \left[\frac{Au_n}{Au_n}\frac{n}{n+n_n}\right]' \\ &= \frac{[Au_n n]'\big(Au_n(n+n_n)\big) - Au_n n[Au_n(n+n_n)]'}{(Au_n(n+n_n))^2} \end{aligned} \tag{30}$$

Substituting (29) in (30)

$$[\alpha(z)]' = f_1(z)\alpha^2(z) + f_2(z)\alpha(z) \tag{31}$$

Where

$$f_1(z) = -CK_{iz}/u_n^2(z)A(z) \tag{32}$$

$$f(z) = \frac{CK_{iz}}{u_n^2(z)A(z)} - \frac{\omega_{wall}}{u_n(z)A(z)} \tag{33}$$

The equation (30) is a first order non-linear ODE with general solution in the form of

$$\alpha(z) = \frac{e^{\int_0^z f_2(x)dx}}{c_1 - \int_0^z f_1(x)e^{\int_0^x f_2(y)dy}dx} \tag{34}$$

When the neutrals' velocity profile u_n, the orifice geometry A and the boundary condition $n(0) = n_0, n_n(0) = n_{n,0}$ are added, (34) can be solved.

It must be noted that the neutrals' velocity profile and the orifice geometry can be quite complicate and therefore it's generally not possible to integrate with elementary functions. Nonetheless, numerical integration can be easily applied to obtain an evaluation of the solution.

Once α is found, plasma and neutrals density profile and current density are easily deduced.

Knowing the value of extracted current from the cathode, the current and current density are calculated from (7).

3. Erosion

Physical sputtering of wall material in high-density plasma region can be caused by multiple phenomena: light-particles sputtering, erosion of the structural elements of the wall, chemical erosion, impurities and many others. Nevertheless, in an environment rich of high-energy ions, one of the main contributors to the erosion may be ion bombardment. The sputtering yield Y curves exist for a variety of materials; however only fitted curve are available for such low potential ($\sim 10-18V$). Therefore, high degree of error is expected($\sim 40\%$). For tungsten the yield is [9][17]:

$$\begin{aligned} Y(\bar{\varepsilon}_i) &= \exp\{-38.744[4.3429\log(\bar{\varepsilon}_i) - 9]^{-0.5} + 8.101\} \\ \bar{\varepsilon}_i &= \varepsilon_i/e \end{aligned} \tag{35}$$

The axial ion flux is deduced from (16), while the radial ion flux is calculated using the density profile and the radial velocity calculated in previous sections. As the channel erode, flux reaching the wall is:

$$(nu_\perp)\cdot\hat{\boldsymbol{n}} \tag{36}$$

With $\hat{\boldsymbol{n}}$ being the vector normal to the orifice wall.

The plasma potential is found using direct integration with the use of a boundary condition at $\varphi(0) = \varphi_0$ (the initial condition φ_0 is given from the 0D insert model), the plasma resistivity η deduced from the quantities calculated from the model.

$$\varphi' = \eta j_e + \frac{\nabla P_e}{ne} - \frac{m_e \nu_{ei}}{ne^2}(enu_{i,z}) \tag{37}$$

The ratio to erosion depth is deduced following [9], assuming that only singly charged ions with energy $\varepsilon_i = e\varphi$.

$$\frac{\Delta h}{R} = \sqrt{1 + \frac{2\Delta t}{R}\frac{AW}{\rho N_{AV}}\big(nu_{i,\perp}\big)Y(\bar{\varepsilon}_i)} - 1 \tag{38}$$

4. Neutrals' velocity profile

This model strongly relays on an assumed velocity profile. And as effort is being delivered in a correct estimation of its nature, a simple case can be evaluated to understand how the neutrals' velocity affects the plasma and erosion behaviour.

4.1. Simplified Poiseuille's flow

As done in all but two-dimensional numerical model, the neutrals' velocity is modelled as a Poiseuille's flow. Furthermore, the thermal gradient is assumed negligible when compared to the density gradient. The neutrals' velocity is:

$$u_n = -\frac{R_0^2 kT_i}{8\zeta}\nabla n_n \tag{39}$$

The mass balance for neutrals states that:

$$\nabla[n_n u_n] = \dot{n} \tag{40}$$

Equation (40) is generally solved with numerical techniques, in this work the homogenous case is

solved and used as further simplification. With use of (3942), the equation (40) simply becomes:

$$[n_n n'_n]' = 0 \tag{41}$$

Which allows for a general solution in form of:

$$u_n(z) = \frac{-c_3}{2\sqrt{c_2 + c_3 z}} \tag{42}$$

$$u_n(exit) = u_{n,end}$$

$$u_n(0) = u_{n,0}$$

$$u_{n,end} = \sqrt{\gamma RT},\ \gamma = 5/3 \tag{43}$$

The flow of "heavy particles" is described by equation (27). The ion flux on the wall is assumed to oppose and equal the flux of neutrals entering the orifice. Every time a neutral undergoes ionization, a neutral is lost but an ion is gained. This implies that, overall, the heavy particles flux is only up and downstream the orifice.

Expanding (16) to include the electric field, the flux is controlled by four terms:

$$nu_{i,z} \approx \frac{ne}{m_i \nu_{in}} E_z - \frac{eT_i}{m_i \nu_{in}} [n]' - \frac{m_e \nu_{en}}{m_i \nu_{in}} \frac{j_e}{e} + nu_n \tag{44}$$

The electric field and the electric drag work in opposition making its sum negligible[9]; the density gradient has little effect and therefore the ion flux is largely dragged by the neutrals flux, allowing us to approximate $u_i \approx u_n$, and if $n \ll n_n$, the flow of heavy particles fluid can be approximated as (42).

Figure 3 shows a comparison with this model, the two-dimensional computational model of Mikellides et al. [9] and the observed erosion.

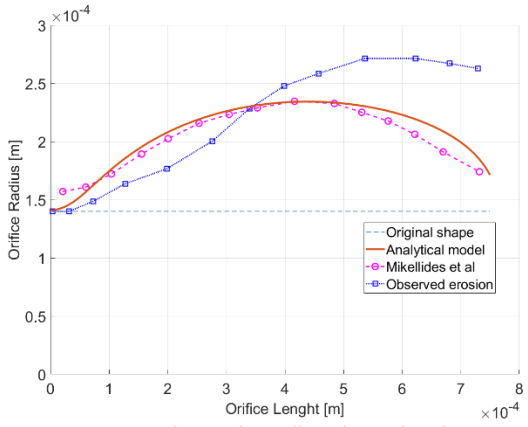

Figure 3 – Comparison of predicted erosion for NHC after 220h.

The nature of the model does not take into account the two-dimensional flow pattern in regions at the orifice entrance and exit. Likely, as the fluid flow inside the orifice, strong density gradient exists in both axial and radial direction, "protecting" the upstream section of the channel from the ion flux on the wall. Howbeit, other aspects of sputtering have to be considered whenever high-density, long-life plasma devices are designed. It is not only because particles sputtered off the walls will constitute a source of contamination of the plasma - changing HCs operational, but also because a small contamination of the plasma with heavy particles could give rise to a substantial sputtering due to the relatively much higher yields of the heavier particles [16]. This phenomenon could, potentially, explain the pattern of the eroded orifice at the downstream exit. It is, however, not yet included in this work.

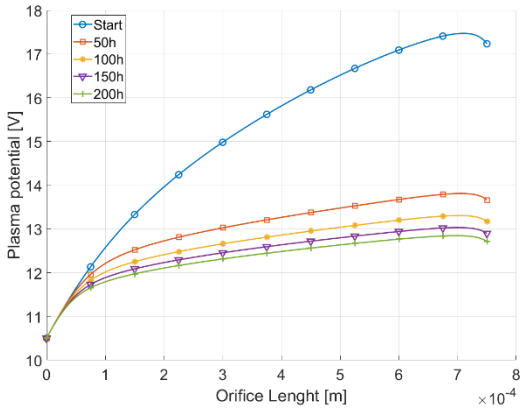

Figure 4 – Calculated plasma potential drop as the channel is eroded.

As the orifice changes shapes, the potential profile drops as seen in Figure 4 . This is believed to be related to the current density relaxation in the middle section of the orifice, which led to a reduction of the resistive electric field in the region. As the potential decreases and stabilizes along the whole channel, the erosion rate effectively decreases slowing down as the channel changes shape.

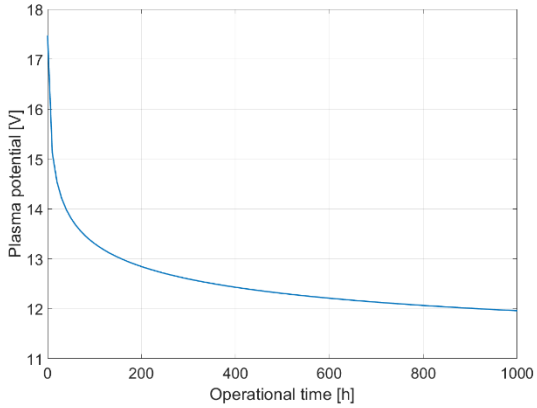

Figure 5 – maximum plasma potential drop over time.

The plasma potential is high at the beginning, which leads to a high erosion rate. Simulation suggests that the erosion is stronger at the beginning of the operations, and then, as the plasma potential drops, it greatly reduces. In figure 5, the maximum potential is shown in time. The early drop of plasma potential suggests that the erosion is very active at the early stages of the operations, to then reduce drastically as the channel expands, and finally

become negligible after a few thousands hours. Figure 6 describe a long-life prediction showing how most of the erosion is concentrated in the first hours of operation.

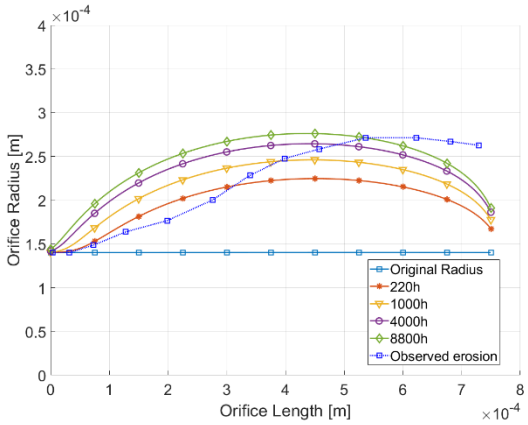

Figure 6 – Calculated erosion for long-life prediction.

5. Sensitivity of heavy particles temperature

Figure 7 shows plasma and neutrals density and plasma potential for the gas temperatures 2500K,3000K, 3500K. Even though the plasma peaks are different, the potential does not seem to be affected much from the gas temperature. The calculated erosion differences after 220h are showed in Figure 8.

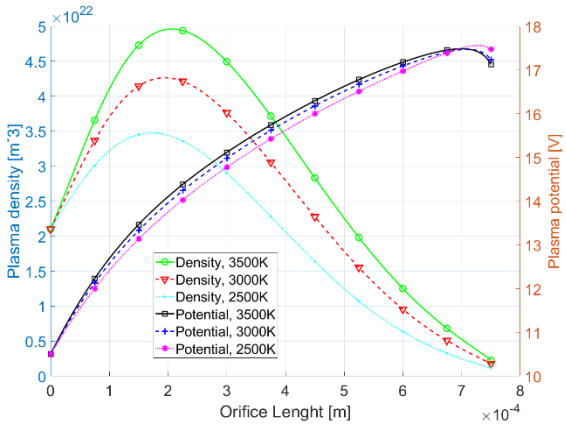

Figure 7 – Plasma density and neutral density at different temperature gas.

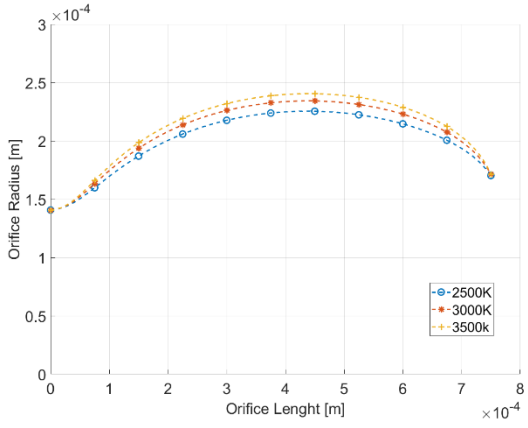

Figure 8 – Calculated erosion after 220h for different gas temperatures

6. Conclusions

In this work, a general analytical solution for simplified steady-state quasi-one dimensional flow model of the partially ionized gas in a neutralizer HC is obtained. It's found that the general solution (34) is not easily solved for general area variation of the orifice channel and numerical integration is used to well approximate the solution. It has been possible to reproduce, qualitatively, the erosion profile of the orifice observed in long-life tests. However, since the model strongly relies on a given neutral profile, more work is needed to achieve a better accuracy. In spite of the great number of simplification made in this work, the model shows a good agreement with the more complex two-dimensional numerical model of [9]. This model is not a direct improvement of the ones found in literature, but the approach is different; and while the fully two dimensional numerical approach is probably more accurate in terms of physical aspect, it is also very expensive both in development and in running time. This work, much simpler, is very easy to reproduce and much faster to run. Useful in the case of preliminary design where many many simulations are required for optimization.

In addition, at the present state the model runs the global mode once, and the retrieved quantities are used to run iteratively the orifice model described. It's likely that as the orifice is eroded, the pressure at the insert, and species temperature changes, and with them the potential and erosion profile, especially in long-time erosion. This will require new boundary condition and re-run of global model to take in account the new orifice geometry. This feature is not yet implemented.

Despite it being a work in progress, we believe the model to be a quick and easy tool to use for orifices investigation, design, life-time and cathode performances.

7. Acknowledgments

The research has been carried out at Southampton University in a collaboration between Alma Sistemi SRL and Mars Space ltd in the frame of the H2020 Marie Curie Research and Innovation Staff Exchange PATH project (Grant#734629).

References

[1] C. J. Wordingham, P.-Y. C. R. Taunay, and E. Y. Choueiri, "Theoretical Prediction of the Dense-Plasma Attachment Length in an Orificed Hollow Cathode List of Symbols."

[2] J. E. Polk *et al.*, "Validation of the NSTAR Ion Propulsion System on the Deep Space One Mission: Overview and Initial Results*."

[3] D. M. Goebel and I. Katz, "Fundamentals of Electric Propulsion: Ion and Hall Thrusters."

[4] C. Charles, “Plasmas for spacecraft propulsion,” *J. Phys. D. Appl. Phys.*, vol. 42, no. 16, p. 163001, Aug. 2009.

[5] D. Mihailova *et al.*, “Geometrical features in longitudinal sputtering hollow cathode discharges for laser applications,” *J. Phys. D. Appl. Phys.*, vol. 45, no. 16, p. 165201, Apr. 2012.

[6] J. T. Guðmundsson, “Ionized physical vapor deposition (IPVD): Technology and applications,” 2007.

[7] Grant#734629, “PATH - Plasma Antenna TecHnologies.” Horizion 2020 - MSCA - RISE 2016.

[8] A. Avzakharchenco Sjnesterenco, “THE MODEL AND CALCULATION OF HOLLOW CATHODE EROSION.”

[9] I. G. Mikellides and I. Katz, “Wear Mechanisms in Electron Sources for Ion Propulsion, I: Neutralizer Hollow Cathode,” *J. Propuls. Power*, vol. 24, no. 4, pp. 855–865, Jul. 2008.

[10] I. Katz, J. R. Anderson, J. E. Polk, and J. R. Brophy, “One-Dimensional Hollow Cathode Model,” *J. Propuls. Power*, vol. 19, no. 4, pp. 595–600, Jul. 2003.

[11] G. Sary, L. Garrigues, and J.-P. Boeuf, “Hollow cathode modeling: I. A coupled plasma thermal two-dimensional model,” *Plasma Sources Sci. Technol.*, vol. 26, no. 5, p. 055007, Mar. 2017.

[12] J. Polk *et al.*, “An overview of the results from an 8200 hour wear test of the NSTAR ion thruster,” in *35th Joint Propulsion Conference and Exhibit*, 1999.

[13] A. Sengupta, J. R. Brophy, and K. D. Goodfellow, “Status of the extended life test of the Deep Space 1 flight spare ion engine after 30,352 hours of operation,” Jul. 2003.

[14] G. Sary, L. Garrigues, and J.-P. Boeuf, “Hollow cathode modeling: II. Physical analysis and parametric study,” *Plasma Sources Sci. Technol.*, vol. 26, no. 5, p. 055008, Mar. 2017.

[15] I. Mikellides, I. Katz, M. Mandell, and J. Snyder, “A 1-D model of the Hall-effect thruster with an exhaust region,” in *37th Joint Propulsion Conference and Exhibit*, 2001.

[16] P. H. Larsen and M. T. Elford, “The mobilities of xenon ions in xenon and the derived charge transfer cross section for $Xe^{+}(^{2}P_{3/2})$ ions in xenon,” *J. Phys. B At. Mol. Phys.*, vol. 19, no. 4, pp. 449–461, Feb. 1986.

[17] R. P. Doerner, “Low-energy sputtering yields of tungsten and tantalum,” *J. Vac. Sci. Technol. A Vacuum, Surfaces, Film.*, vol. 23, no. 6, pp. 1545–1547, Nov. 2005.